Sustainable structural health monitoring using field programmable gate array (FPGA) technology

B.G. Farfan[1], M. Azarbayejani[2], A.I. El-Osery[4] and M.M. Reda Taha[1,3]

[1] Dept. of Electrical and Computer Engineering, University of New Mexico, Albuquerque, NM, USA
[2] Dept. of Civil Engineering, University of Texas Pan American, Edinburg, TX, USA
[3] Dept. of Civil Engineering, University of New Mexico, Albuquerque, NM, USA
[4] Dept. of Electrical Engineering, New Mexico Tech, Socorro, NM, USA

ABSTRACT: An innovative field application of a structural health monitoring (SHM) system using Field Programmable Gate Array (FPGA) technology, wireless communication and renewable energy is presented in this article. The novel SHM system was installed in summer 2009 to monitor a reinforced concrete (RC) bridge on Interstate I-40 in Tucumcari, New Mexico, USA. The newly installed system is powered using solar energy. The integration of FPGA and solar power technologies make it possible to remotely monitor infrastructure with limited access to power. This article describes the design and installation process of the SHM system on bridge 7937 Tucumcari, New Mexico. A 3-D finite element (FE) model of the bridge was developed and calibrated using static loading test. The sensor network, data acquisition system and monitoring center are explained. The sustainable energy source throughout solar cells is also explained. The proposed monitoring system and software can replace prescheduled bridge inspection protocols to provide a robust maintenance system, thus reducing human intervention significantly.

1 OVERVIEW

Structural health monitoring (SHM) is the term used to describe the technical activities necessary to “keep an eye” on infrastructure. SHM incorporates the necessary work to deploy sensors on the structures and to communicate and analyze data acquired by these sensors to detect damage and provide reliable strategies for structural maintenance and repair. Deploying efficient SHM systems on bridges can provide early warning about potential damage. Moreover, continuous monitoring of bridges might enable switching from the current classical ‘schedule-based’ maintenance to ‘condition-based’ maintenance where maintenance is tied to structural performance. Such switch can result in saving millions of dollars by focusing our resources to maintenance needs (Adam 2007).

The basic components of SHM include data acquisition, data processing, damage detection, damage pattern recognition and structural prognosis to evaluate the structural life. One important aspect in data processing is the need for an efficient signal de-noising technique. While many researchers described SHM systems in the context of anomaly detection (cf. Bukkapatnam et al. 1999), major SHM research was focused on feature extraction and pattern recognition. A hierarchical structure of SHM systems was described by Worden & Dulieu-Barton (2004). Moreover, Farrar et al. (2004) provided an in-depth analysis of the status and needs for damage prognosis to estimate the remaining life of infrastructure. Essential damage prognosis research demonstrated that a critical issue to sensing and data acquisition is the need to capture response on varying length and time scales.

The SHM design and installation portrayed in this paper has been developed on bridge 7937 on Interstate 40 (I-40) in the city of Tucumcari, New Mexico, USA. This bridge consists of five reinforced concrete (RC) K-Frame girders (Figure 1). The K-Frames form three spans; 42 ft, 104 ft and 42 ft. Each K-frame has a rectangular RC cross-section whose depth varies along the length of the bridge.

Figure 1. K-Frames in bridge 7937.

During the last two decades since the bridge was constructed, the size and weight of trucks passing over I-40 have increased dramatically. It is expected that the moment and shear demand of the current traffic load might exceed bridge capacity. To ensure that bridge 7937 falls within the state limit requirements of AASHTO 2006, four fiber reinforced polymer (FRP) strips has been installed on the bridge. Figure 2 shows FRP strips installed on bridge 7937.

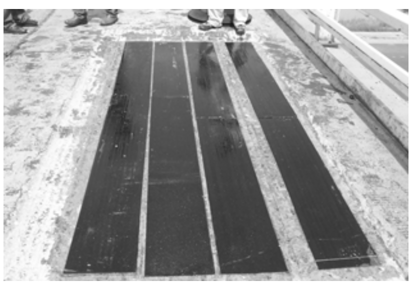

Figure 2. FRP sheets installed on bridge 7937.

2 STRUCTURAL HEALTH MONITORING SYSTEM

The SHM system to monitor bridge 7937 includes accelerometers and strain gauges along with thermocouples. Twenty accelerometers were used to extract structural dynamic information at different locations on the bridge. The acceleration data was used to extract damage feature(s) which can differentiate between healthy and damage conditions and enable warnings when the bridge is damaged. The SHM system for bridge 7937 was designed to operate using a field programmable gate array (FPGA) data acquisition system. This system is denoted as smart data acquisition system (SDAQ) for its capability to implement intelligent damage detection and damage pattern recognition algorithms. SDAQ system can thus make decision to communicate the sensing data for further analysis or to cleanse it to save computational resources and communication overhead. The system can also connect wirelessly to the Worldwide Web and transfer synchronized monitoring data using HTTP and FTP protocols.

The location of the sensors was determined based on structural analysis of the bridge by identifying the most critical structural locations. This was done by using a three-dimensional finite element (FE) model of the bridge, as shown in Figure 3. First, the model was validated using field measurements during a load test of the bridge. The bridge model was then used to simulate the structural behavior of the bridge and determine critical locations that were more prone to damage. With this information, sensor locations on the bridge were identified. A methodology for identifying the optimal sensor network was developed by the authors and is described elsewhere (Azarbayejani et al. 2008).

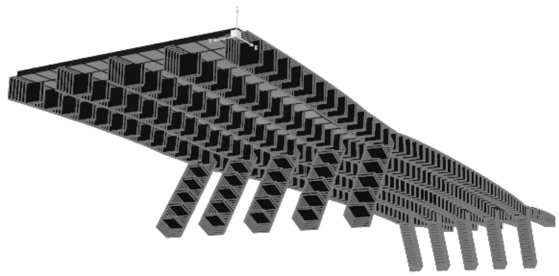

Figure 3. Three dimensional FE Model for bridge 7939 used to identify critical bridge locations.

Furthermore, strain sensors were used on FRP sheets to monitor the possible de-bonding between FRP sheets and concrete deck of the bridge. Thermocouples were used at different locations on top and bottom of the bridge to measure temperature and determine temperature gradient. Figure 4 illustrates a schematic of the SHM system installed on bridge 7937 and all its components as well as the wireless communication system operability.

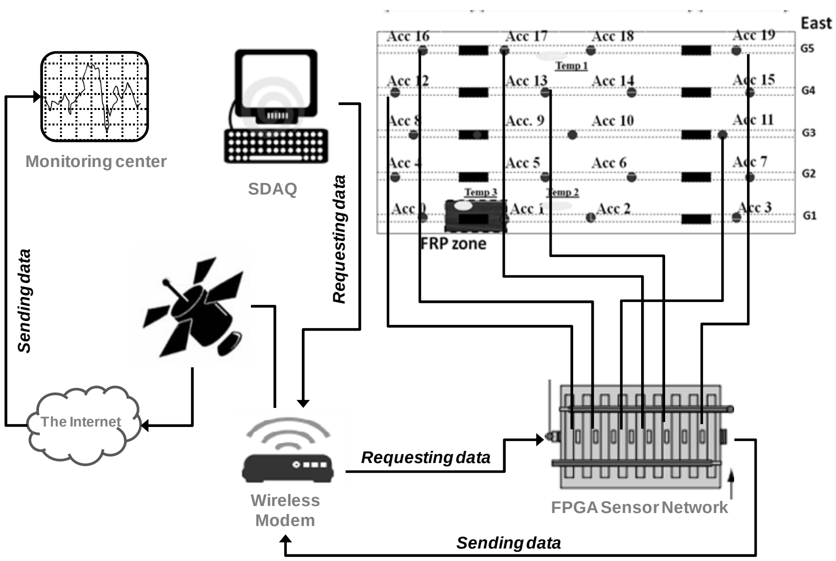

Figure 4. Schematic representation of SHM system with components as designed for bridge 7937.

3 INSTALLATION OF SHM SYSTEM

After testing and calibrating all the components of the SHM system on a model truss bridge and ensuring system ability to detect damage, the SHM system was brought to the bridge location in Tucumcari and was installed on bridge 7937.

3.1 Sensors and SDAQ installation

The installation of the sensors network and SDAQ began with the allocation of the electronic component housing which consists of an outdoor-rated steel box enclosure (Nema 4). The box enclosure houses the data acquisition, wireless modem, the power inverter and solar panel batteries. After installation of the component's housing, metal hangers were attached to the bridge using drills. Hangers were also used to create guides for accelerometer cables from different points on the bridge to the steel box. Accelerometers were installed using stainless steel plates that were specially designed and tested before installation. The stainless steel plates were anchored to the bottom of the bridge deck in very close proximity to the girders, and accelerometers were then attached to the steel plates.

Later, a conduit with a small electrical box was made to pass the cables from strain gauges attached on the FRP strengthened zone on top of the bridge to the data acquisition (DAQ) box at the bottom. After installing all the accelerometers and attaching them to the SDAQ system, the strain gauges were installed on the FRP sheets to monitor debonding of FRP sheets from the concrete surface. Environmentally protected strain gauges produced by Vishay, Inc. were used. The strain gauges were installed following standard installation techniques. Special epoxies were used to attach the strain gauges to the FRP sheets. The strain gauges were left for 24 hours before connecting to the SDAQ. All strain gauges were covered and the wires from them were attached to the cables which transmit the signals from the strain gauges to the SDAQ system. Concrete was cast over the bridge deck area where the FRP strengthening was applied and the strain gauges were installed as shown in Figure 5. Moreover, four thermocouples were installed on the top surface and the underside of the bridge to measure the thermal gradient of the bridge.

Figure 5. Concrete casting over area of bridge deck strengthened with FRP after installing strain gauges.

3.2 Solar power system installation

The solar power system was designed to provide the total energy consumption to operate the SDAQ in Tucumcari, New Mexico, Latitude: 35° 10' 18" N - Longitude: 103° 43' 27" W. The design consists of an initial energy load estimation of the system that needs to be satisfied, the photovoltaic (PV) array design and an autonomy system to backup days of autonomy. The solar power system incorporates a wireless communication modem, the DAQ modules, a current inverter device and a time controller. Based on the operation requirements of 8 hours of continuous energy supply, the daily energy consumption (Ec), presented in Table 1, was estimated.

Table1. Energy load

Device	Power (W)	Daily Operation time (hr)	Daily Consumption (Whr)
Wireless Modem	4.2	8	33.6
DAQ module	48	8	384
Inverter	7.8	8	62.4
Time controller	1.4	24	33.6
		E_c *(Whr/day)*	513.6

The solar power system has been designed to meet the power demand described above and to power the SDAQ system for operability in 1 day of autonomy. Based on the respective design parameters, the different components of the PV system were determined. For this particular case, we designed the system over the inverter type 375 Watt TRIPP-LITE and used the battery type 8A27-DEKA AGM. Kyocera KC130TM solar panel was also used. Figure 6 shows the electrical diagrams for the respective PV system installed to operate the SHM system.

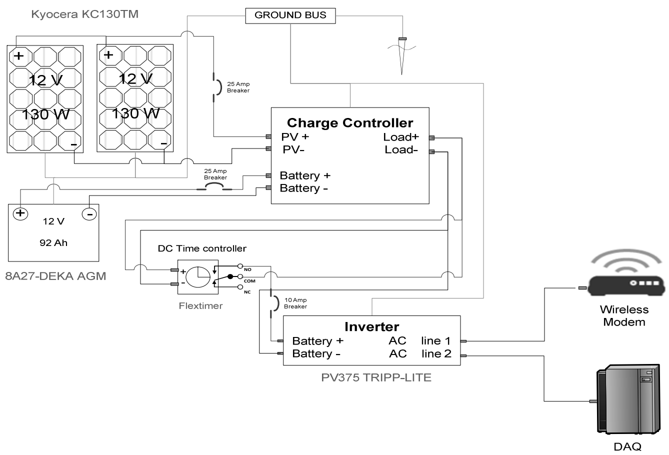

Figure 6. Layout of proposed PV system for 1 day of autonomy.

Solar power was successfully installed and is timed to work 8 hours every day. Special time for data download during low wireless activity is also scheduled. Figure 7 shows the installed solar power panels that provide clean renewable energy to the SHM system and their connection to the monitoring system.

Figure 7. Solar power system installed on bridge 7937 provides clean renewable energy for SHM.

Upon completion of the installation of all sensors on the bridge surface, they were connected through their cables to the SDAQ system housed in the steel box and located underneath the bridge. The SDAQ was connected wirelessly throughout a data modem to the Worldwide Web. The solar power system components such as inverter, charger, time controller and batteries were also integrated and installed in the same housing with the SDAQ system.

4 MONITORING CENTER

4.1 Monitoring user interface

With the SDAQ system and wireless modem, the user can monitor the bridge wirelessly through the World Wide Web. The DAQ system is programmed in such a way that provides the user an easy graphical user interface (GUI) to monitor the bridge and obtain data from all the sensors installed on the bridge. Moreover, the GUI gives the user the ability to control the SDAQ remotely by choosing the data and time frame to be saved on the DAQ device. The rate of data acquisition can be changed from 2000 Hz to 50,000 Hz. In addition, the user has the ability to change the "Excitation Voltage" requirements needed for strain gauge modules and the "Configuration" of strain gauges in Wheatstone bridge from "Half-Bridge" to "Full Bridge".

Special software is developed for reading and analyzing this data. The software called SMART-SHM is composed of two programs that are designed to run on typical PCs. The first program, SMART-SHM-START.EXE, allows the user to view the data files downloaded from the bridge as "raw data". The second program, called SMART-SHM-DAMAGE.EXE, is designed for damage feature extraction and damage detection. The user has the ability to view all the sensors on the bridge and to display the synchronized data from the bridge for up to 4 sensors at a time. SMART-SHM-START allows the user to perform basic analysis of the data. Four types of analysis are available. They includes fast Fourier transform (FFT) and Wavelet transform (WT). The software also allows the user to view a down-loaded-sample wavelet transform of any desired sensor. SHM-SMART-DAMAGE, was designed to perform damage feature extraction using WT and FFT and to display the history of the bridge damage feature(s). Figure 8 provides a snapshot of SMART-SHM-START software.

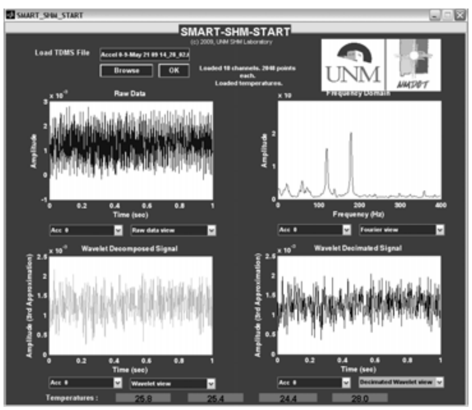

Figure 8. Snapshot of SMART-SHM-START software shows its four data views.

4.2 Data analysis for damage detection

The first thing required to perform damage analysis and damage detection is to train the system based on available data gathered from the bridge during a specific period of time. The training dataset is used to establish the boundaries of the damage feature (based on FFT or WT). The boundaries were established at 99.7% probability. After the training dataset is loaded, a new dataset can be loaded. Here, two different methods are used for detecting damage on the bridge:

First, Fast Fourier Transform (FFT) of the bridge signals is used. When damage occurs to the bridge, the main frequency components of the bridge may change and therefore the frequency components of the acceleration signals will change. Since the bridge has very large stiffness and mass, a small amount of damage may not be able to change the major frequency components of the bridge. The maximum frequency component considered here was limited to 45 Hz since the signals with higher frequencies usually represent noise. In the training part of this method, the maximum frequency of signals at each sensor is computed for each training dataset and the mean value of all datasets are used for the training process. The upper and lower bounds for the healthy state of the bridge are calculated based on 99.7% probability. At any later time, the new observations are compared to the bounds established early, based on the bridge time histories, and damage is considered to occur when new observations go beyond the statistical bounds.

Second, the energy of signals calculated in the wavelet domain is used as a damage feature to differentiate between healthy and damage states of the bridge. The acceleration signal is decomposed into approximation and detail signals with low and high frequency components, respectively using WT. The decomposed signal of $x'(n)$ at level p can be computed as

$$x'(n) = \sum_{k=-\infty}^{\infty} a_{p,k} . \phi_{p,k}(n) + \sum_{j=1}^{p} \sum_{k=-\infty}^{\infty} d_{p,k} . \varphi_{p,k}(n) \tag{1}$$

where $x'(n)$ is the decomposed signal. Moreover $\phi_{p,k}(n)$ and $\varphi_{p,k}(n)$ are the scaling and wavelet basic functions, respectively. In this SHM system for the bridge, the scaling and wavelet functions are selected for the Daubechies db4 mother wavelet. The approximation coefficients $a_{p,k}$ and $d_{p,k}$ the detail coefficients are calculated as

$$a_{p,k} = 2^{(-p/2)} \sum_{n} x(n) \phi(2^{-p} n - k) \tag{2}$$

$$d_{p,k} = \sum_{n} x(n) \varphi_{p,k}(n) \tag{3}$$

The signals were down-sampled from 2 kHz to 400 Hz sampling rate. The third approximation of the acceleration signal is then used to compute the damage feature λ representing the energy of the third approximation signal computed over a time window as

$$\lambda = \sum_{k} (a_{3,k})^2 \tag{4}$$

Experimental and analytical investigations, Reda Taha et al. (2004) and McCuskey et al. (2006) proved the ability of the proposed damage metric λ to detect and quantify damage occurrence in bridges and multi-story structures respectively. Using the energy of the wavelet decomposed signals, the training datasets were computed. The mean value and 99.7% boundaries were established. For any new dataset obtained from the bridge, if the energy of signals calculated in the wavelet domain at the location of each sensor passes the statistical boundaries, the bridge might be experiencing damage near the location of that sensor. Figure 9 presents a snapshot of the SMART-SHM-Damage software showing the mean and statistical bounds for the Fourier transform damage feature at sensor 1. The frequency mean value of all training datasets is around 20 Hz (as shown in Figure 9) while the lower and upper limits will be between -5 and 40 Hz. It is apparent that all the frequencies are within the established range that confirms the healthy state of the bridge. The system is currently in use by the State of New Mexico.

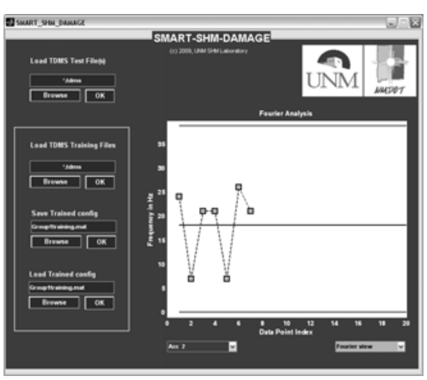

Figure 9. Snapshot of SMART-SHM-DAMAGE shows frequency damage feature at sensor 1.

Since the bridge is in healthy condition and in service, the efficiency of the system was only examined using a finite element model calibrated using field measurements. Further information on SHM system efficiency evaluation can be found elsewhere (Azarbayejani 2009).

5 CONCLUSIONS

This paper described the installation and operation of this new SHM system for monitoring bridge 7937 in Tucumcari, New Mexico. The new system is powered with clean renewable solar energy with one day autonomy. The SHM system for bridge 7937 was designed to operate using a field programmable gate array (FPGA) data acquisition system. This system is designed to wirelessly connect and operate so the bridge can be fully monitored over the Worldwide Web. Two damage features are computed from the data acquired on the bridge using fast Fourier and wavelet transforms. Statistical bounds are established based on historical healthy data. New datasets observed from the bridge are analyzed and a damage detection analysis is performed.

6 ACKNOWLEDGMENT

This work is funded by Federal Highway Administration (FHWA) Contract Number CO5102 to New Mexico Department of Transportation (NMDOT) through the Innovative Bridge Research and Deployment (IBRD) program. The authors greatly acknowledge this support. Special thanks to Aaron Reinhardt and Mohammad Jalalpour from UNM, Luke Graham and David Bonal from National Instruments (NI) and NMDOT District 4 Engineers and field crew.

7 REFERENCES

AASHTO. 2006. LRFD *Bridge Design Specifications, Manual for Condition Evaluation of Bridges. Interim revisions*, *Second Edition*. Washington, D.C: American Association of State Highway and Transportation Officials.

Adam, DE. 2007. *Health Monitoring of Structural Materials and Components: Methods and Applications*. John Wiley & Sons, Inc.

Azarbayejani, M, El-Osery, A., Choi, KK and Reda Taha MM. 2008. Probabilistic Approach for Optimal Sensor Allocation in Structural Health Monitoring. *Smart Materials and Structures*, 17: paper # 055019.

Azarbayejani, M. 2009. Optimal sensor Placement for Structural Health Monitoring (SHM) with a Field Application on a RC Bridge. PhD Dissertation, Department of Civil Engineering, University of New Mexico, Albuquerque, New Mexico, USA.

Bukkapatnam,, STS, Kumara, SRT and Lakhtakia, A. 1999. Analysis of Acoustic Emission Signals in Machining. *ASME Journal of Manufacturing Science and Engineering*, 121: 568-576.

Farrar, CR, Sohn, H, Hemez, FM, Anderson, MC, Bement, MT, Cornwell, PJ, Doebling, SW, Lieven, N, Robertson, AN and Schultze, JF. 2004. Damage Prognosis: Current Status and Future Needs. Los Alamos National Lab Report, LA-14051-MS.

McCuskey, M, Reda Taha, MM, Horton, S and Baca, TJ. 2006. Identifying Damage in ASCE Benchmark Structure using a Neural-Wavelet Module. In *Proc.of the International Workshop on SHM*, 421-428.

Reda Taha, M, Noureldin, A, Osman, A and El-Sheimy, N. 2004. Introduction to the Use of Wavelet Multi-Resolution Analysis for Intelligent Structural Health Monitoring. *Canadian Journal of Civil Engineering*, 31: 719-731.

Worden, K and Dulieu-Barton, JM. 2004. An Overview of Intelligent Fault Detection in Systems and Structures. *Structural Health Monitoring*, 3: 85-98.